

# Synthesis of Nanostructured Hydroxides and Oxides of Iron: Control Over Morphology and Physical Properties

Babita Baruwati, K. Madhusudan Reddy, and Sunkara V Manorama<sup>\*,†</sup>

Nanomaterials Laboratory, Indian Institute of Chemical Technology, Hyderabad 500 007, India

S. S. Madhavendra

Center for Electron Microscopy, Indian Institute of Chemical Technology, Hyderabad 500 007, India

**This paper reports on the surfactant-assisted synthesis of nanotubes and nanorods of  $\beta$ -FeOOH and hence  $\alpha$ -Fe<sub>2</sub>O<sub>3</sub> (hematite) with remarkable stability against temperature under different reaction conditions. Characterization and a comprehensive study of their nanosized properties are carried out by powder X-ray diffraction, thermal analysis, transmission electron microscope, and vibrating sample magnetometer. Upon calcination at 300°C,  $\beta$ -FeOOH nanostructures transform to  $\alpha$ -Fe<sub>2</sub>O<sub>3</sub> with some change in morphology. The samples convert to layered rod-like structures and further into some sort of a disc resembling stacked structures upon heat treatment. Even for magnetic fields up to 10 000 G, the magnetization curves for the nanotubes/nanorods of hematite do not attain the saturation magnetization. All the materials exhibit a very low coercivity even at room temperature and hence are potential materials for magnetic applications.**

## I. Introduction

THE last few years have witnessed a sudden interest in obtaining semiconductor nanocrystals in the form of particles, rods, tubes, etc. both for fundamental research and technical applications, due to their strong size-dependent properties and excellent chemical processibilities.<sup>1–4</sup> The control over morphology to generate anisotropic nanostructures is recognized as a very important issue as nanometer-sized materials in the form of particles, rods, or wires exhibit many unique properties associated with their inherent shape anisotropy.<sup>5</sup> In particular, transition metal oxides constitute one of the most fascinating classes of inorganic solids, as they exhibit a wide variety of structures, properties, and phenomena. For example, ferromagnetic nanowires exhibit unique and tunable magnetic properties because of the shape anisotropy and small wire dimensions. In fact, all the relevant magnetic properties of nanoparticles are functions of particle size, shape, and surface chemistry. These particles could be oriented and arranged to improve their magnetic properties and thus widen their potential uses.

Nanoparticles of magnetic oxides, including most representative ferrites, have been studied for many years for their application as magnetic storage media, ferrofluids, and electrode material for Li rechargeable batteries.<sup>6</sup> Also, hydroxides of iron-like  $\beta$ -FeOOH find applications in Li cell batteries,<sup>7</sup> industrial usages as harmless pigment in cosmetics,<sup>8,9</sup> and also as a precursor for hematite.<sup>10</sup> In particular, the hematite form of iron

oxide ( $\alpha$ -Fe<sub>2</sub>O<sub>3</sub>) is an antiferromagnetic oxide that is widely used in pigment industry, steel industry, in catalytic processes,<sup>11</sup> a raw material for synthesis of  $\gamma$ -Fe<sub>2</sub>O<sub>3</sub>, a sensor,<sup>12</sup> and many magnetic applications. Nanostructuring of these materials is known to make it superparamagnetic; that is, above a certain temperature, the material no longer exhibits hysteresis. Various techniques have been developed for the synthesis of one-dimensional (1-D) nanostructures such as template-assisted synthesis,<sup>13</sup> colloidal,<sup>14</sup> micellar, solvothermal synthesis, and molecular assemblies.<sup>15</sup> Among them, generally, the nanorod synthesis necessitates temperatures > 160°C, but very recently cetyl trimethyl ammonium bromide (CTAB), a cationic surfactant, has shown promise in the synthesis of PbO and ZnO nanorods by template-assisted synthesis at comparatively lower temperatures.<sup>16</sup>

With the above background, in the present paper, we report on the synthesis of nanostructured  $\beta$ -FeOOH and thereby  $\alpha$ -Fe<sub>2</sub>O<sub>3</sub> with different architectures by a not so elaborate process but simply by controlling the synthesis parameters. Here, a series of experiments have been performed using different reagents to obtain nanosized iron oxide rods at room temperature, and the magnetic properties have been studied on a vibrating sample magnetometer (VSM).

## II. Experimental Procedure

A surfactant-assisted synthesis procedure is adopted to prepare iron hydroxide/iron oxide nanorods/nanotubes with a high aspect ratio, i.e., length to width ratio using different reducing agents and varying the reaction conditions, and these are described in the following sections.

A set of four similar experiments have been carried out. In each set, 100 mL NaOH (3M) solution was taken, to which 2.14 g (6 mmol) of CTAB was added and stirred vigorously for 15 min to dissolve CTAB in NaOH completely. Subsequently, to each set, 0.10 g (0.8 mmol) of anhydrous FeCl<sub>2</sub> (Sigma Aldrich Chemical Co., Bangalore, India) was added. Instantaneously, a light green-colored precipitate appears, which turns reddish orange as the reaction proceeds further. The next step was to use different known hydrolyzing agents and observe their influence on the morphology of the final products. To accomplish this, 1 mL of hydrazine, 0.144 g of glucose, and 1 mL of triethylamine were added to the first, second, and third sets, respectively, followed by vigorous stirring for 2 h. The fourth set, consisting of CTAB in NaOH with FeCl<sub>2</sub>, was directly transferred to a teflon-lined autoclave and maintained at 120°C for 10 h. After the reactions were completed, the precipitates were washed repeatedly with distilled water and finally with methanol and dried at ambient temperature and pressure. The samples will henceforth be referred to as H, G, T, and HT for the samples prepared from hydrazine hydrate, glucose, triethylamine, and hydrothermal treatment, respectively.

L. Klein—contributing editor

Manuscript No. 20886. Received August 17, 2005; approved February 16, 2006.

This work was supported by Department of Science and Technology, New Delhi and CSIR, India.

IJCT Communication No.: 040510.

\*Life Member, Indian Ceramic Society.

†Author to whom correspondence should be addressed. e-mail: manorama@iict.res.in

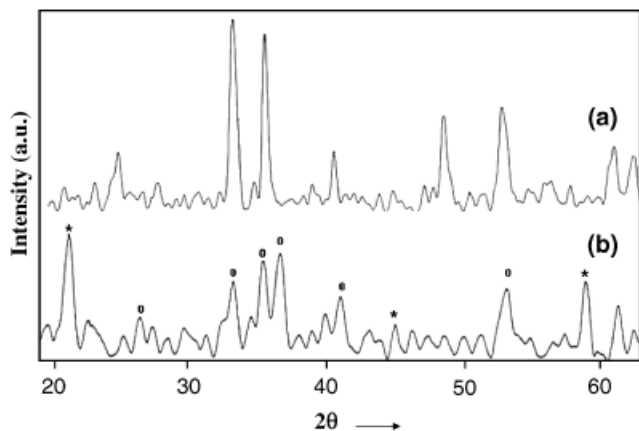


**Fig. 1.** Representative powder X-ray diffraction pattern for the as-synthesized sample (b) and after calcinations at 350°C (a).

Thermogravimetric and differential thermal analysis (TG-DTA, Mettler Toledo, Star<sup>c</sup> system) of the as-prepared samples was carried out under air, from room temperature to 800°C at 5°C/min, to assess the thermal stability and phase changes, if any, taking place during heating. The synthesized nanosized  $\beta$ -FeOOH and  $\alpha$ -Fe<sub>2</sub>O<sub>3</sub> have been characterized for their structure and morphology by powder X-ray diffraction (XRD, Siemens D5000, Munich, Germany) and transmission electron microscopy (TEM, JEOL JEM 100 CX, Tokyo, Japan), coupled with a selected area electron diffraction facility. The XRD spectra were recorded using CuK $\alpha$  radiation ( $\lambda = 1.5406$  Å) source. The intensity data were collected over a  $2\theta$  range 2°–60° in the step scan mode (counting time 0.5 s; step width 0.045°). The average crystallite size of the samples was estimated with the help of the Scherrer equation using the full-width at half-maxima of all prominent intensity peaks. For TEM studies, the samples were dispersed in ethanol by ultrasonication and then loaded over formvar-coated copper grids. The grids were air dried before recording the micrographs.

The magnetic properties associated with these nanomagnetics have been investigated by a VSM (Lakeshore 7400, Lakeshore, OH) at room temperature with applied field up to 10 000 G.

### III. Results and Discussion

Figures 1(a) and (b) show the representative XRD patterns of the as-synthesized material (b) and after calcination at 350°C (a). From the XRD data, it is found that the as-synthesized samples are predominantly  $\beta$ -FeOOH (JCPDS Card No. 34-1266), along with some amounts of  $\gamma$ -FeOOH. Fourier transform infrared studies also confirm these observations. We have observed absorption bands at 1624, 845, and 695  $\text{cm}^{-1}$  along with a band at 1158  $\text{cm}^{-1}$ , confirming that the as-synthesized sample is mainly  $\beta$ -FeOOH with a small amount of  $\gamma$ -FeOOH.

To increase the crystallinity and to observe temperature-assisted phase changes, the samples were calcined at various temperatures. Figure 1(a) shows the powder XRD pattern for hematite nanorods, in agreement with bulk hematite (JCPDS Card No. 33-664). The crystallite sizes were calculated from the Scherrer formula applied to the XRD data using the  $d$  value of the most intense peaks. The crystallite sizes were calculated to be about 8–10 nm for the uncalcined samples and 12–13 nm for the calcined samples.

Indeed, Figs. 2(a)–(d) show TG and DTA traces that are rather similar to each other between 200° and 300°C. The endothermic peak observed in this region is tentatively ascribed to the transformation of  $\beta$ -FeOOH to  $\alpha$ -Fe<sub>2</sub>O<sub>3</sub>, and the mass loss of ~10%–12% (expected 10.5%) observed under DTA peaks confirms the proposed transformation.

Figures 3(a)–(d) show typical TEM micrographs of all the as-prepared samples. From the TEM micrograph, it can be observed that samples G and HT have a rod-like structure,  $H$  exhibits a tubular structure, while  $T$  exhibits a needle-like morphology. The lengths of the nanorods and tubes are about 1200 nm, with an aspect ratio of 15, and for the needles the typical lengths are around 700 nm, with a similar aspect ratio of 14. From a combination of XRD, TG-DTA data, and TEM

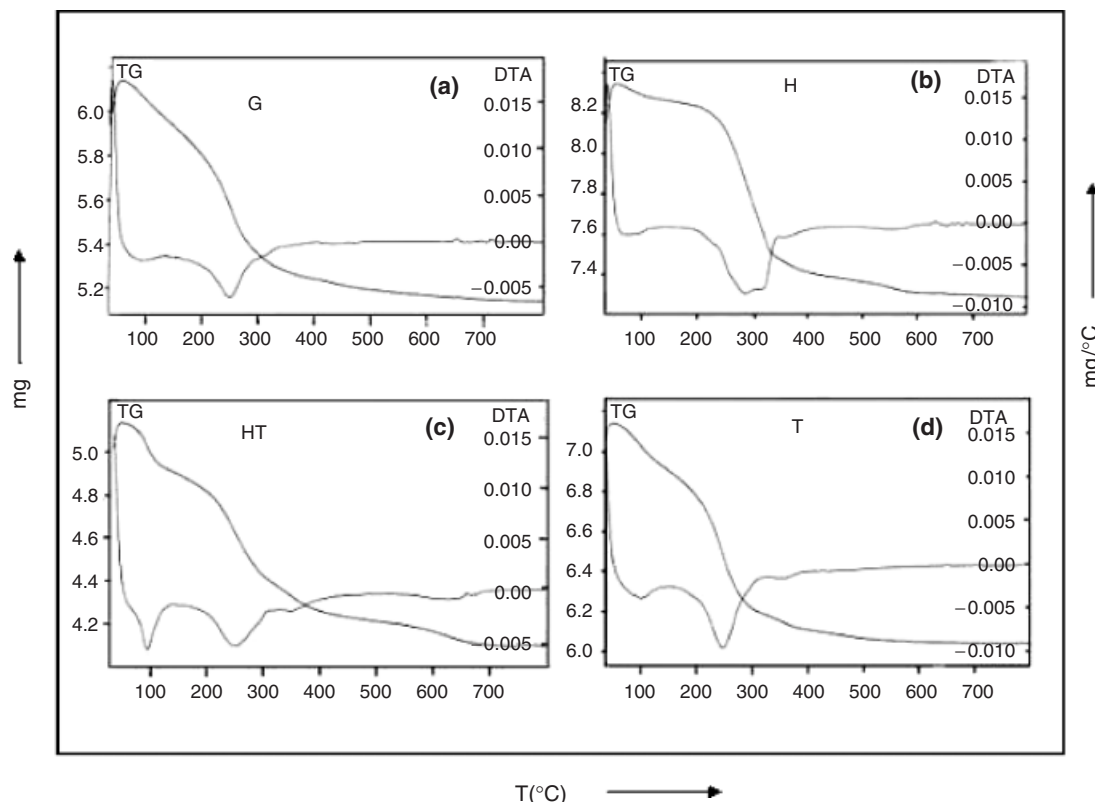


**Fig. 2.** Thermogravimetric–differential thermal analysis traces for the samples synthesized by (a) glucose, (b) hydrazine hydrate, (c) hydrothermal treatment, and (d) triethylamine.

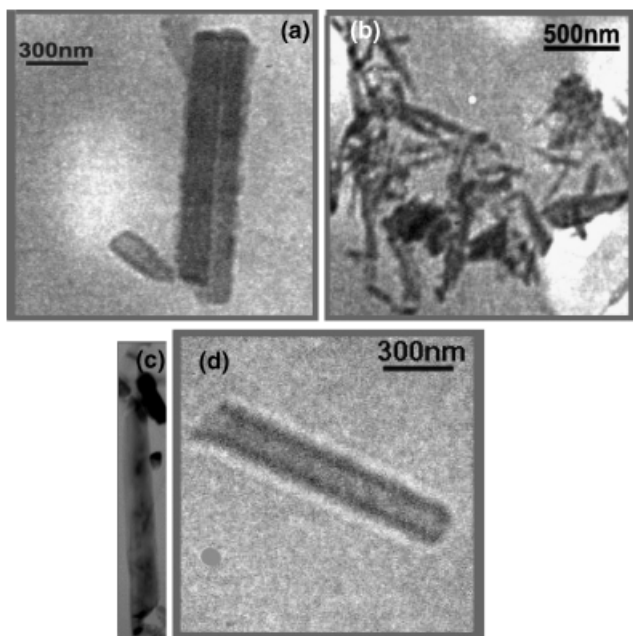


**Fig. 3.** Transmission electron microscopy pictures of the as-prepared samples (a) glucose, (b) triethylamine, (c) hydrothermal treatment, and (d) hydrazine hydrate. Samples prepared from glucose and hydrothermal treatment show nanorod morphology, hydrazine hydrate shows tubular morphology, while that of triethylamine shows needle-like morphology.

micrographs, it is observed that after calcination at 350°C, the samples transform to  $\alpha$ -Fe<sub>2</sub>O<sub>3</sub> without any change in the morphology. The rod-like structure in the as-synthesized sample shows some indication of becoming hollow or layered as seen from the TEM micrographs after heat treatment at 350°C. These rod-like structures appear to be closed at the ends. The response to the high-temperature treatment shows structure stability up to nearly 600°C for the HT sample and a total col-

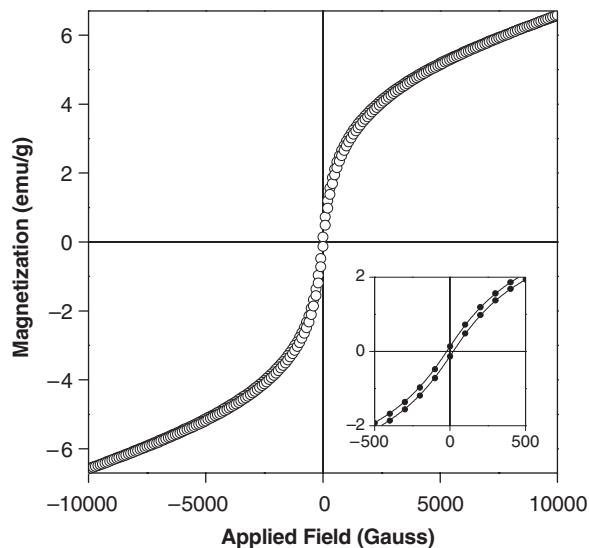


**Fig. 5.** Representative magnetic moment (emu/g) versus field (G). Hysteresis plots for the  $\alpha$ -Fe<sub>2</sub>O<sub>3</sub> nanorod/tube samples recorded at room temperature for a field of 10 kG. The inset shows the coercivity of the sample.

lapse after 700°C. Figures 4(a) and (b) show representative transmission electron micrographs of the HT and G samples calcined at 350°C that depict morphological stability. Figure 4(c) shows the representative TEM micrograph of an HT sample calcined at 700°C that shows the collapse of the rod-like structures. Here, structures resembling disks seem to be formed as seen in the TEM picture. Figure 4(d) shows the TEM picture of the sample T after heat treatment at 700°C, confirming the stability of the sample even after the high-temperature treatment.

All synthesized nanostructures were analyzed for their magnetic properties by a VSM. We did not observe much difference in the magnetization values for the different samples. Figure 5 shows the representative magnetization plot for the nanorods

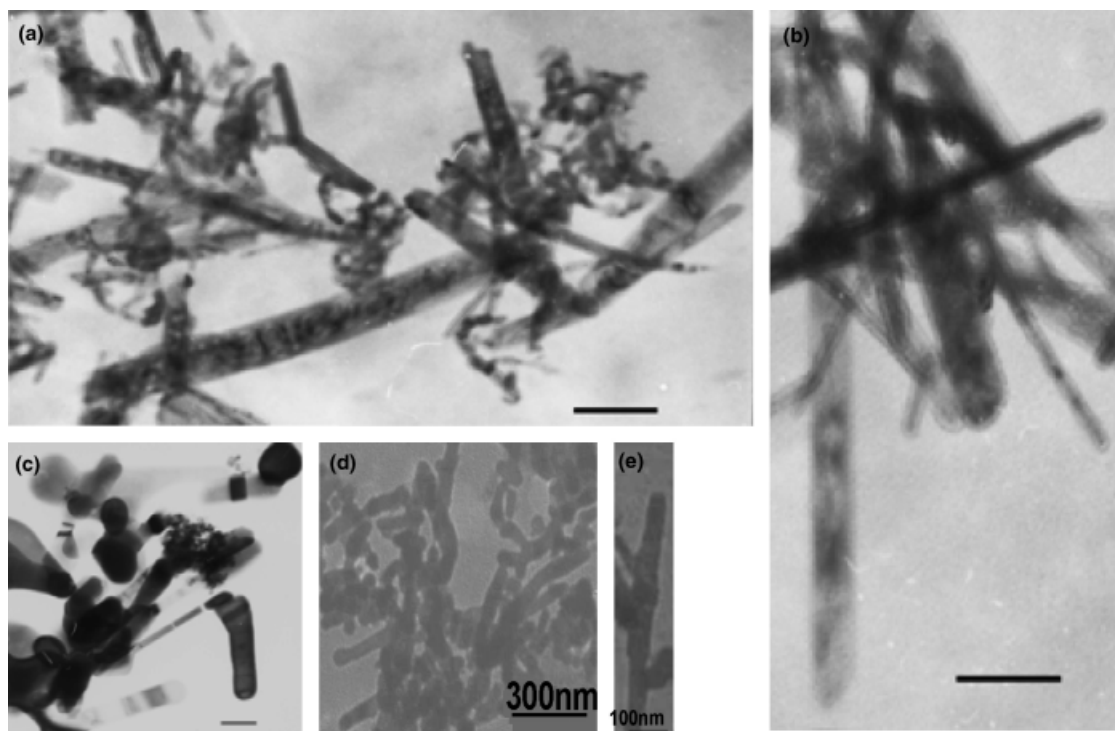


**Fig. 4.** (a) and (b) Transmission electron micrographs of the samples calcined at 350°C and (c)–(e) calcined at 700°C. (c) Shows that the rod morphology breaks down at 700°C for the sample synthesized by the hydrothermal route. (d) and (e) Show that the structure is retained for the samples synthesized via hydrolysis even after calcining at 700°C (sample used T). (Scale bar: 50 nm for a–c)

(sample G) measured at 300 K with an applied magnetic field of 10 000 G. The inset shows the coercivity, which is almost negligible, around 8–10 G. The low coercivity is a characteristic feature of fine particle magnets, which is a consequence of the superparamagnetic response. The curves exhibit a steep increase in magnetization with increasing magnetic field, demonstrating typical magnetization characteristics of the superparamagnetic material, and the magnetization does not saturate even at 10 000 G magnetic field. This could possibly be attributed to the elongated geometry of the synthesized materials that tends to enhance and favor the coupling interaction between particles, preventing the magnetization saturation even at such high magnetic fields.

### (1) Mechanism

Based on our observations, a probable mechanism to explain the formation of iron oxide nanotubes/rods/needles by the synthetic procedure deployed could be put forth as follows: starting with iron chloride and maintaining the alkaline pH results in the conversion of the chloride into hydroxide. This first step results in a possible electrostatic interaction existing between the hydroxide and the CTAB, a cationic surfactant, favoring the formation of a complex in the precursor. It is expected that on addition of the hydrolyzing agent, very fine particles of oxide are formed that serve as seeds for the growth of the nanostructures. The hydroxide–CTAB chloride complex would be adsorbed on these iron oxide seed particles. This adsorption passivates the surface seed nuclei, resulting in functionalized sites on the surface directing the growth of the particles. Under the condition maintained as the reaction progresses, the growth proceeds along the active sites directed by the hydroxide–surfactant complexes, resulting in the formation of elongated nanostructures in the form of rods and tubes. It is to be noted that we do not observe stable structures when no hydrolyzing agents like triethylamine, hydrazine hydrate, or glucose are used. In case of hydrothermal treatment, we do obtain rods but in this case the temperature acts as the key factor for the formation of rods. In comparison, the rods formed by the hydrothermal method show lower stability with temperature than those obtained by using a hydrolyzing agent. This also proves that the hydrolyzing agents conform to structure and make the architecture stable.

Some insights into the detailed mechanism could be speculated based on the analysis of the experimental procedure adopted and the observations made. CTAB is known to form spherical, cylindrical, etc., micelles depending on the solution conditions.<sup>17</sup> In our case, we observe that by simply using different hydrolyzing agents, different 1-D nanostructures of the oxide are obtained. This means that the different conditions are provided by the variety of hydrolyzing agents used. Using NaOH along with CTAB would effect the formation of micellar structures. It has also been speculated that the role of NaOH would simply not be just to effect the formation of micellar structure but also act as a catalyst or micellar structure modifier.<sup>18</sup> This speculation gains support from our observation that without NaOH, we observe only nanoparticles. We believe that because of the electrostatic interaction of the inorganic precursor and the cationic surfactant CTAB, different conformational inorganic–surfactant composites may form, which may serve as templates for the formation of different morphologies. Further, there may be a possibility of a kinetic effect of the hydrolyzing agents apart from the above-mentioned templating role. Different hydrolyzing agents will hydrolyze FeCl<sub>2</sub> at different rates and hence the growth rate of the particles will be affected. This

might have enabled us to obtain the FeOOH/Fe<sub>2</sub>O<sub>3</sub> nanostructures with different morphologies having remarkable stability against temperature.

## IV. Summary

The study undertaken brings out the following conclusions:

1. Successfully synthesized  $\beta$ -FeOOH and  $\alpha$ -Fe<sub>2</sub>O<sub>3</sub> in the form of tubes, rods, and needles starting from FeCl<sub>2</sub> and using CTAB as the cationic surfactant.
2. The synthetic procedures and various reagents have been standardized to obtain the oxides of the desired morphology.
3. The stability of the structures to heat treatment has been established and comparison made among the different procedures adopted.
4. All these nanostructures exhibit the superparamagnetic effect with low coercivity as seen from the room-temperature hysteresis studies.

## Acknowledgments

The authors are grateful to Mr. C. S. Murthy, Incharge, CIL, Hyderabad Central University, India, for his help in carrying out the magnetic measurements.

## References

- <sup>1</sup>J. Hu, M. Ouyang, P. Yang, and M. Lieber, "Controlled Growth and Electrical Properties of Heterojunctions of Carbon Nanotubes and Silicon Nanowires," *Nature*, **399**, 48–51 (1999).
- <sup>2</sup>K. Woo, J. Hong, S. Choi, H. W. Lee, J. P. Ahn, C. S. Kim, and S. W. Lee, "Easy Synthesis and Magnetic Properties of Iron Oxide Nanoparticles," *Chem. Mater.*, **16** [14] 2814–8 (2004).
- <sup>3</sup>L. Vayssieres, N. Beermann, S. E. Lindquist, and A. Hagfeldt, "Controlled Aqueous Chemical Growth of Oriented Three-Dimensional Crystalline Nanorod Arrays: Application to Iron (III) Oxides," *Chem. Mater.*, **13** [2] 233–5 (2001).
- <sup>4</sup>D. Weller and A. Moser, "Thermal Effect Limits in Ultrahigh Density Magnetic Recording," *IEEE Trans. Magn.*, **35**, 4423–39 (1999).
- <sup>5</sup>G. Bottoni, D. Cadolfo, A. Cecchetti, and F. Masoli, "The Effect of Multiple Anisotropies in Fine Particles," *J. Magn. Magn. Mater.*, **45** [1] 91–9 (1984).
- <sup>6</sup>K. Padhi, K. S. Nanjundaswamy, C. Masquelier, S. Okada, and J. B. Goodenough, "Effect of Structure on Fe<sup>3+</sup>/Fe<sup>2+</sup> Redox Couple in Iron Phosphates," *J. Electrochem. Soc.*, **144**, 1609–13 (1997).
- <sup>7</sup>Y. Xiong, Y. Xie, S. Chen, and Z. Li, "Fabrication of Self Supported Patterns of Aligned  $\beta$ -FeOOH Nanowires by a Low Temperature Solution Reaction," *Chem. Eur. J.*, **9**, 4991–6 (2003).
- <sup>8</sup>H. Katsuki and S. Komameni, "Microwave-Hydrothermal Synthesis of Mono-dispersed Nanophase Agr-Fe<sub>2</sub>O<sub>3</sub>," *J. Am. Ceram. Soc.*, **84** [10] 2313–7 (2001).
- <sup>9</sup>R. M. Cornell and U. Schwertmann, *The Iron Oxides, Structure, Properties, Reactions, Occurrence and Uses*. VCM, Weinheim, Germany, 1996.
- <sup>10</sup>T. Ihsikawa, R. Katoch, A. Yasukawa, K. Kandori, T. Nakayama, and F. Yuso, "Influences of Metal ions on the Formation of  $\beta$ -FeOOH Particles," *Corrosion Sci.*, **43**, 1727–38 (2001).
- <sup>11</sup>A. Brown, J. Hargreaves, and B. Rijnerse, "A Study of the Structural and Catalytic Effects of Sulfation on Iron Oxide Catalysts Prepared from Goethite and Ferrihydrite Precursors for Methane Oxidation," *Catal. Lett.*, **53**, 7–13 (1998).
- <sup>12</sup>L. Huo, W. Li, L. Lu, H. Cui, S. Xi, J. Wang, B. Zhao, Y. Shen, and Z. Lu, "Preparation, Structure and Properties of Three Dimensional Ordered  $\alpha$ -Fe<sub>2</sub>O<sub>3</sub> Nanoparticles Film," *Chem. Mater.*, **12**, 790–4 (2000).
- <sup>13</sup>M. Cao, C. Hu, Y. Wang, Y. Guo, C. Guo, and E. Wang, "A Controllable Synthetic Route to Cu, Cu<sub>2</sub>O and CuO Nanotube and Nanorods," *Chem. Commun.*, 1884–5 (2003).
- <sup>14</sup>C. B. Murray, S. Sun, W. Gaschler, H. Doyle, T. A. Betley, and C. R. Kagan, "Colloidal Synthesis of Nanocrystals and Nanocrystal Superlattices," *IBM J. Res. Dev.*, **45**, 47–56 (2001).
- <sup>15</sup>D. Chen and X. Jiao, "Solvochemical Synthesis of  $\alpha$ -Fe<sub>2</sub>O<sub>3</sub> Particles with Different Morphologies," *Mater. Res. Bull.*, **36**, 1057–64 (2001).
- <sup>16</sup>H. Zhang, D. Yang, Y. Ji, X. Ma, J. Xu, and D. Que, "Low Temperature Synthesis of Flower like ZnO Nanostructures by Cetyltrimethylammonium Bromide-Assisted Hydrothermal Process," *J. Phys. Chem. B*, **108**, 3955–8 (2004).
- <sup>17</sup>V. K. Aswal, P. S. Goyal, and P. Thiyagarajan, "Small-Angle Neutron Scattering and Viscosity Studies of CTAB/NaSal Viscoelastic Micellar Solutions," *J. Phys. Chem. B*, **102**, 2469–73 (1998).
- <sup>18</sup>D. H. Chen and C. H. Hsieh, "Synthesis of Nickel Nanoparticles in Aqueous Cationic Surfactant Solutions," *J. Mater. Chem.*, **12**, 2412–5 (2002). □